Letter Vol. 6, No. 1 / January 2019 / Optica 115

Surface plasmon polaritons on curved surfaces

Ana Libster-Hershko, Roy Shiloh, and Ady Arie*

Department of Physical Electronics, Faculty of Engineering, Tel-Aviv University, Tel-Aviv 69978, Israel
**Corresponding author: ady@post.tau.ac.il*

Received 20 August 2018; revised 12 November 2018; accepted 2 December 2018 (Doc. ID 342699); published 18 January 2019

While the motion of a classical particle bounded to a surface depends only on the local curvature, the dynamics of a quantum particle depends also on the mean surface curvature. Its influence can be experimentally observed using surface plasmon polaritons (SPPs), which are naturally surface-bounded waves. Owing to the similarity between the Schrödinger and the paraxial Helmholtz equations, this system can be used to readily examine quantum phenomena. In this work, we experimentally show a new guiding mechanism based on this quantum effect using the surface curvature of a book-cover structure, whereas in the case of an inverse book cover with the same local curvature but inverted mean curvature, the SPPs rapidly diffract. Additionally we show that, by longitudinally bending the book cover, the propagating mode width can be dynamically controlled.

https://doi.org/10.1364/OPTICA.6.000115

The motion of a particle on a curved surface was theoretically studied in the context of quantum mechanics by da Costa [1] more than 35 years ago. In general, for each point on the surface, we can define two circles that are tangent to it, with radii R_1 and R_2. da Costa showed that the equation of motion of a quantum particle bounded to a surface is different from that of a classical particle, in that the tangent part of the wave depends not only on the metric of the surface, defined by the product $(1/R_1) \times (1/R_2)$, but also on the mean curvature, $(1/2) \times (1/R_1 + 1/R_2)$. The existence of geometric potential for a quantum particle constrained to a curved frictionless surface that vanishes for a classical particle is a controversial problem in quantum mechanics, since there were difficulties in defining such a potential [2–4]. Geometrical potential was demonstrated in condensed matter [5] and nanoscale systems [6]. The propagation dynamics of quantum particles can be studied using optical or plasmonic beams by relying on the similarity between the Schrödinger and the paraxial Helmholtz equations [7]. This caused a revival in the study on curved-space geometric potentials in recent years. Specifically, the propagation of light beams along thin dielectric curved surfaces was studied theoretically [8–12] and experimentally [13–16]. However, surface plasmon polaritons (SPPs) require no additional dielectric layers, since they are two-dimensional waves that propagate at a metal-dielectric interface, so the definition of the geometric potential is well posed [17]. In virtue of their inherent two-dimensional nature, they provide an ideal environment for studying this phenomenon [18,19]. This advantage of SPPs for studying the propagation on a book-cover surface was theoretically recognized by Della Valle *et al.* [17], but up till now, experimental studies of the unique features of plasmonic propagation along curved surfaces were not reported.

In this Letter, we study a plasmonic curved-space propagation, and in particular, the propagation of SPPs on a structure with the shape of a book cover [1,17]. Such a structure is obtained by a plane bent around the surface of a cylinder of radius R_1 and an angular aperture 2θ. Here the radii of the two tangent circles are R_1 and $R_2 = \infty$; hence the Gaussian and mean potential are 0 and $1/R_1$, respectively. Though classically such a structure should not exhibit guiding properties, it is effectively a finite square potential well for quantum particles, thereby supporting bound quantum modes. An inverse book-cover structure provides a potential hill due to the sign change of the mean curvature, and quantum particles would not be confined. The existence of a mode on the book-cover structure and its absence on an inverse structure provides the simplest and most direct evidence of the mean potential's role, but despite the many years that have passed since it was proposed [1], it has never been tested experimentally up till now, either with plasmonic waves, or with any other type of waves.

The experimental setup is presented in Fig. 1. Continuous-wave 1.064 μm laser light is grating-coupled to the silver (Ag)-air interface, generating SPPs on the curved book-cover structure. The plasmon's intensity distribution is subsequently measured using a near-field scanning optical microscope (NSOM, Nanonics MultiView 2000). The grating was designed to generate a Gaussian plasmonic mode [20] with 3 μm waist, to match the desired guided mode's width. To fabricate the curved-surface plasmonic structure, we defined a photolithographic mask containing clear and opaque lines, intended for inverted and normal book-cover structures, respectively. The lines are 5 μm wide and 150 μm in length. Then, we follow a standard photolithography process started with a silicon substrate, coated with AZ1518 photoresist by spin-coating at 3000 RPM for 40 s, followed by a prebake on a hotplate heated to 115°C for 90 s. The photoresist is then exposed and developed. In the final step, we place the sample on a preheated hotplate at 130°C for 90 s. At this temperature, the resist begins to reflow [21], and the book-cover structure is formed. We have found that the structure formation

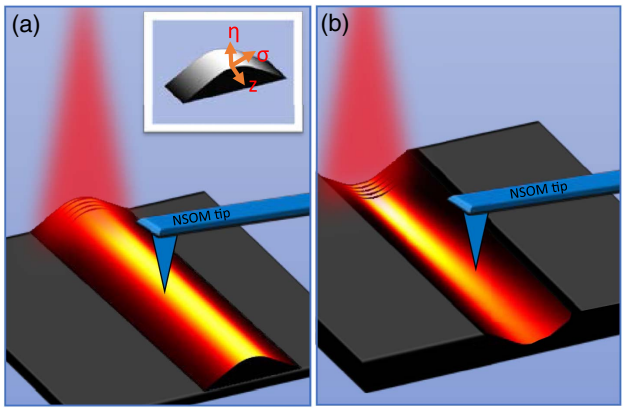

Fig. 1. (a) Experimental setup for the book-cover structure. Inset, curvilinear coordinates definition; (b) experimental setup for the inverse book cover. The plasmonic beam is excited from free space through a grating coupler, and an NSOM tip measures the intensity distribution.

is repeatable and reproducible. In the last step, the structure is coated with 100 nm of Ag, and a Raith IonLine focused ion beam working at 35 kV and 90 pA is used to mill coupling gratings directly on the book-cover structures. The grating was milled into the Ag layer using focused ion beam. We can neglect the propagation losses, since the propagation length of SPPs on the interface between Ag and air at 1064 nm is about 1 mm, much larger than all the distances we measure in our experiments.

The propagating mode is simulated using an effective-index mode solver [22], using the geometric potential of the curved surface. One may derive it as follows. First, Maxwell's equations are solved in curvilinear coordinates (σ, η, Z) [see inset of Fig. 1(a)] on the cylindrical surface of the book cover, and a multiple-scale asymptotic analysis is applied. The equation for the SPP envelope becomes [17]

$$i\frac{\lambda}{2\pi}\frac{\partial A_{\mathrm{spp}}}{\partial Z} = -\frac{\lambda^2}{8\pi^2 n_{\mathrm{spp}}}\frac{\partial^2 A_{\mathrm{spp}}}{\partial \sigma^2} + V_{\mathrm{eff}}(\sigma)A_{\mathrm{spp}}, \tag{1}$$

where A_{spp} is the SPP envelope, λ is the wavelength, $n_{\mathrm{spp}} = [\varepsilon_d\varepsilon_m/(\varepsilon_d+\varepsilon_m)]^{1/2}$ is the SPP's effective index, and $\varepsilon_d, \varepsilon_m$ are the relative dielectric permittivity constants in the dielectric and metal, respectively. $V_{\mathrm{eff}}(\sigma)$ is the geometrical potential

$$V_{\mathrm{eff}}(\sigma) = \begin{cases} -\frac{\lambda n_g}{4\pi R_1}\sqrt{-\frac{1}{\varepsilon_d+\varepsilon_m}}, & |\sigma| \le R_1\sin(\theta/2) \\ 0, & |\sigma| > R_1\sin(\theta/2) \end{cases}, \tag{2}$$

with R_1 cylinder's radius. The equivalence in the form of Eq. (1) and the paraxial wave equation in curvilinear coordinates [11,16] allows us to find the topological refractive index n of the surface:

$$n = \sqrt{n_{\mathrm{spp}}^2 - 2n_{\mathrm{spp}}V_{\mathrm{eff}}}. \tag{3}$$

Thus, the geometric potential, owing to the surface curvature, induces a change in the refractive index. We emphasize here that this change does not come from any variation in the metal or dielectric materials, which have the same properties in the central curved region, as well as in the flat regions that surround it. We used n for the middle layer of an equivalent two-dimensional symmetric slab waveguide in our mode solver, where the first and last layers represent the flat surfaces with the plasmonic refractive index of n_{spp}. We verified our calculations with a commercial FDTD mode solver (Lumerical Solutions). Simulation results for the propagating mode found by Lumerical and the mode solver are presented in Figs. 2(a) and 2(b), respectively. According to the mode solver, there are no propagating modes in the case of the inverse book-cover surface, as expected from theory.

To test the theoretical predictions, we fabricated and experimented with three structures: a book cover, an inverse book cover, and a combined structure, as follows.

In the first experiment, we demonstrate a guided mode on a 150 μm long book-cover structure. Figures 2(a)–2(g) show good agreement between simulation and measurements. The slight asymmetry observed in Fig. 2(c) probably originates from asymmetric collection efficiency of the NSOM fiber tip. The radius of the cylinder is $R = 4.8$ μm, and the length of the chord that is bounding the used segment of the cylinder is 4.17 μm. We show that the profile of the SPPs at the beginning of the propagation (green) and after a propagation of 40 μm (blue) are at the same width and intensity; see Fig. 2(d). Also shown is the topographic measurement of the book cover (red). The green SPP profile was taken 8 μm from the grating because of the scattered sidelobes from it, which are not part of the guided mode. The correlation between the two SPP profiles in Fig. 2(d) is 0.89. In comparison, we measured the SPPs generated by an identical grating on a flat surface, Fig. 2(e), where it can be clearly seen that after a propagation of 50 μm, the SPP profile is broader. The beam's Rayleigh range is 26.5 μm. The dashed black line in Fig. 2(e) shows the width of the theoretical beam. The propagation of the measured beam is slightly tilted with respect to the theoretical beam.

In our second experiment, we investigate an inverse book-cover structure. Here, the mean curvature is opposite that of the regular book cover. Our experimental results in Figs. 2(f)–2(g) verify that SPPs are indeed not guided on this structure. It can

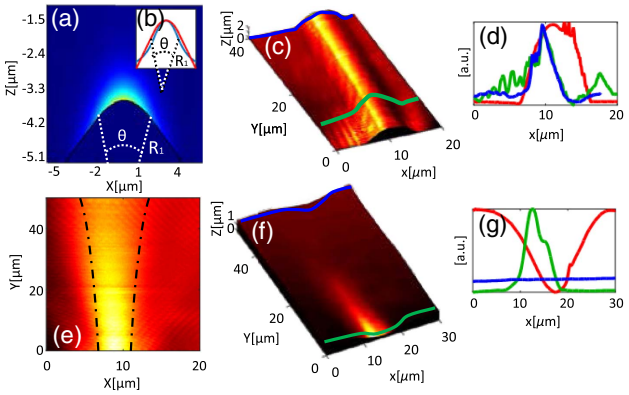

Fig. 2. Simulation and experimental results. (a) Lumerical mode solver result for a book cover structure; (b) geometrical shape of the book-cover structure (red) and the intensity distribution of the plasmonic mode solver (blue); (c) 3D plot of the measured book-cover topography with the intensity of the SPP overlaid; (d) measured topographic profile of the book-cover structure (red) and the intensity distribution of the SPPs at beginning of the propagation (green) and after 40 μm (blue); (e) SPPs measured on a flat surface with a Gaussian grating. Dashed-dotted line defines the theoretical width of a Gaussian plasmonic beam; (f) 3D plot of the measured inverse book-cover topography with the intensity of the SPP overlaid; (g) measured topographic profile of the inverse book-cover structure (red) and the intensity distribution of the SPPs at beginning of the propagation (green) and after 50 μm (blue).

be seen that the SPP width increases dramatically, and the intensity decays to nearly zero over a propagation distance of 50 μm [Figs. 2(f)–2(g)]. This behavior is predicted by theory, and it proves the crucial role of the mean curvature on the SPPs' propagation dynamics.

As a third example, we fabricated a combined structure that contains a book cover and two additional inverse book-cover structures, one on each side, as shown in Fig. 3(a). Here we use a wide coupling grating to couple the SPPs to all three structures simultaneously. As seen in Fig. 3(a), there is a guided SPP on the book-cover structure in the middle, whereas at the edges of the structure, the adjacent inverse book covers, no guided signal exists throughout the entire 50 μm of propagation. This measurement provides an additional proof that a book-cover structure can guide plasmonic beams, but the inverted book cover cannot. The sidelobes in Fig. 3(a) are generated from the rounded corners of the structure. In Fig. 3(b), we show the overlap of the plasmonic profiles and the topographic profile at the beginning and end of the structure. For a single book-cover structure, the rounded curvatures at the edges of the experimentally realized structure are insignificant, since the plasmonic intensity there is negligible. For the inverted book structure, the plasmonic beam exhibits rapid spreading and will therefore reach the region in which the surface is curved in the opposite direction. If this curvature has a large radius, as in the case of Fig. 2(f), it will not be able to "trap" the plasmonic wave, but when it becomes small enough, as in the case of Fig. 3, the plasmonic beam will be localized at the "hills" and repelled from the "valleys" of the structure.

Finally, we show theoretically how to dynamically control the propagating mode on the book cover by longitudinally bending the structure on the (y, z) surface along a constant radius [12]. This bending is mathematically described using the conformal transformation $z + iy = R2 * \exp(v + iu/R2)$. The equation for the SPP envelope [Eq. (1)] becomes [12] (see Supplement 1)

$$i\frac{\lambda}{2\pi}\frac{\partial A_{\mathrm{spp}}}{\partial v} = -\frac{\lambda^2}{8\pi^2 n_{\mathrm{spp}}}\frac{\partial^2 A_{\mathrm{spp}}}{\partial \sigma^2} + V_{\mathrm{eff}}(\sigma)A_{\mathrm{spp}} - \frac{n_{\mathrm{eff}}}{R_2}v(q_2)A_{\mathrm{spp}}, \tag{4}$$

where R_2 is the radius of curvature normal to the y-z plane. The additional potential $n_{\mathrm{eff}}/R_2 \cdot v(q_2)$ describes the variation of the potential well with propagation, $v(q_2)$ being the length of the curved structure from the input point; q_2 is a curvilinear coordinate that is aligned with the surface. By assuming the potential changes slowly during propagation, the adiabatic theorem can be applied [23]. Therefore, along the propagation, for every v value, the SPPs remains in an eigenmode of the system; hence, the output eigenmode depends on the bending radius and structure length, L. For positive radius R_2 [Fig. 4(b)], as the radius increases, the width of the mode is reduced with respect to the width of the mode when $R_2 = \infty$ [Fig. 4(a)]. For the negative radius, Fig. 4(c), the mode width is increased until the book cover does not support a mode anymore. For this radius, there is a cancellation of the potential well. Hence, by changing the radius of the bending, from −0.5 m to 0.5 m, we can control the mode width, as shown in Fig. 4(d) for book-cover structures with the same profile as in Fig. 2(c) that are 150 μm long.

It is important to note that the structures we study here are fundamentally different than the so-called grooved or channel SPP waveguide [24] and wedged SPP waveguide [25,26]. These structures consist of two planar metal-dielectric layers that are connected by a tiny subwavelength radial region, with typical dimensions of several tens of nanometers. The guiding mechanism in those structures is not based on the geometrical potential, but on the increase in the effective index when the two planar interfaces are in close proximity [24]. As a result, the guided mode is tightly confined, with deep subwavelength dimensions, to either the bottom of the groove or the top of the wedge. In contrast to that, the guiding mechanism we study here is based solely on the curvature of the surface, and the dimensions of the curved region and the guided mode are of the wavelength scale. Whereas the groove structure can guide SPPs, the inverted book-cover structure cannot because of the different guiding mechanism: the negative mean curvature means that the geometric potential acts as a potential barrier, and therefore guiding is prohibited, as we showed in Figs. 2(f) and Eq. (3). The inverted book cover starts to guide when the distance between the planar structures on the two sides of the curved region is of the same order as the plasmonic decay in the dielectric, and the corresponding radius of the curvature should be below ∼0.5 μm. Since in our experiment the radius of the inverse book cover was 10 μm, guiding was not observed, and the propagation was controlled by the geometric potential. We also should highlight the differences with respect to dielectric-loaded waveguides on flat surfaces, in which an additional high-index stripe is employed to guide the beam.

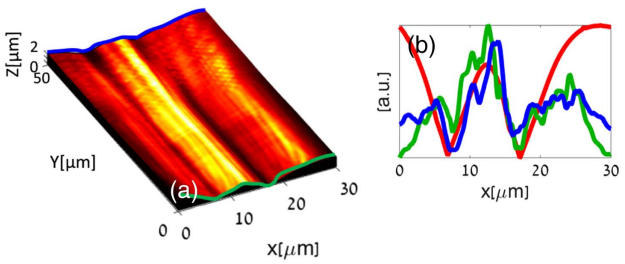

Fig. 3. Experimental results. (a) 3D plot of the measured combined book-cover topography with the intensity of the SPPs overlaid; (b) profile of the combined book-cover structure (red) and the profile of the SPPs as measured with the NSOM at the beginning of the propagation (green) and after 50 μm (blue).

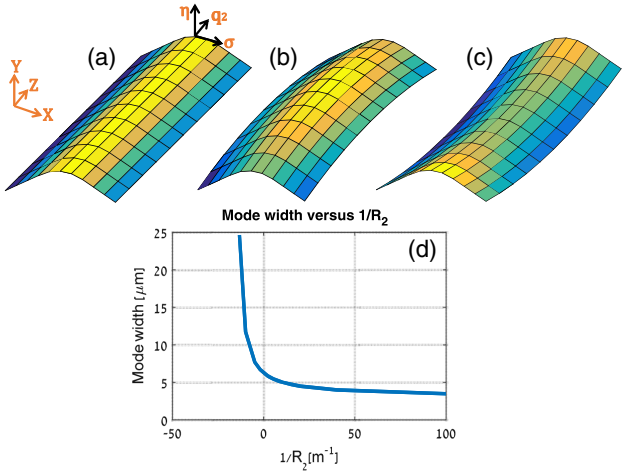

Fig. 4. Longitudinal bending of the book-cover structure. (a) $R_2 = \infty$ with Cartesian and curvilinear coordinates shown; the colors in this figure visualize the bending of the structure; (b) positive R_2; (c) negative R_2; (d) mode width as a function of $1/R_2$ for $L = 150$ μm.

This additional layer is not needed here, but the curved-space waveguide enables direct near-field coupling to the guided mode (which was used here for the NSOM measurements), whereas in a dielectric-loaded waveguide, the high-index dielectric layer prevents direct access to the mode, and only a small fraction of the beam that leaks through the dielectric of the metal can be probed.

In conclusion, we investigated the role of the mean curvature by showing guiding of SPPs on a curved surface with the shape of a book cover. Our experimental observations are in excellent agreement with the theory of a quantum particle confined to curved surfaces, where both the mean curvature and the metric of the surface determines the propagation dynamics, in contrast to classical particles. The ability to fabricate, measure, and control SPPs on curved surfaces opens new research possibilities, enabling experimentation on a variety of quantum phenomena. It can be used to study accelerating beams on curved surfaces [27], to explore the propagation of SPPs on curved graphene surfaces [28,29], to study Bloch oscillations in an array of curved-space waveguides [12], and to realize new types of plasmonic topological optical elements–lenses [30–35], deflectors, diffractive elements, etc.,–in a compact manner by proper curvatures of the metal-dielectric boundary. In addition, these book-cover structures can guide signals between planar metasurfaces [36,37]. Furthermore, it can be used for mimicking general relativity effects, e.g., by constructing analogs of black holes [19] and white holes, and by studying the formation of event horizon and Hawking radiation [38]. Another future prospect is studying the propagation along plasmonic curved lines, as proposed by da Costa [1], where the reduced dimensionality can be reached by forming metal lines on curved dielectric substrate.

Funding. Israel Science Foundation (ISF) (1415/17); Israeli Ministry of Science and Technology.

Acknowledgment. The authors would like to acknowledge Prof. Zhigang Chen for helpful discussions.

See Supplement 1 for supporting content.

REFERENCES

1. R. C. T. da Costa, Phys. Rev. A **23**, 1982 (1981).
2. H. Jensen and H. Koppe, Ann. Phys. (N.Y.) **63**, 586 (1971).
3. M. Ikegami, Y. Nagaoka, S. Takagi, and T. Tanzawa, Prog. Theor. Phys. Suppl. **88**, 229 (1992).
4. N. G. van Kampen and J. J. Lodder, Am. J. Phys. **52**, 419 (1984).
5. V. Vitelli, J. B. Lucks, and D. R. Nelson, Proc. Natl. Acad. Sci. USA **103**, 12323 (2006).
6. C. Ortix, S. Kiravittaya, O. G. Schmidt, and J. van den Brink, Phys. Rev. B **84**, 045438 (2011).
7. D. Dragoman and M. Dragoman, *Quantum-Classical Analogies, The Frontiers Collection* (Springer, 2004).
8. S. Batz and U. Peschel, Phys. Rev. A **78**, 043821 (2008).
9. J. Gravesen, M. Willatzen, and L. C. L. Y. Voon, Phys. Scr. **72**, 105 (2005).
10. J. Gravesen, M. Willatzen, and L. C. L. Y. Voon, J. Math. Phys. **46**, 012107 (2005).
11. G. Della Valle, M. Savoini, M. Ornigotti, P. Laporta, V. Foglietti, M. Finazzi, L. Duò, and S. Longhi, Phys. Rev. Lett. **102**, 180402 (2009).
12. S. Longhi, Opt. Lett. **32**, 2647 (2007).
13. V. H. Schultheiss, S. Batz, A. Szameit, F. Dreisow, S. Nolte, A. Tünnermann, S. Longhi, and U. Peschel, Phys. Rev. Lett. **105**, 143901 (2010).
14. G. Lenz, I. Talanina, and C. M. de Sterke, Phys. Rev. Lett. **83**, 963 (1999).
15. A. Patsyk, M. A. Bandres, R. Bekenstein, and M. Segev, Phys. Rev. X **8**, 011001 (2018).
16. A. Szameit, F. Dreisow, M. Heinrich, R. Keil, S. Nolte, A. Tünnermann, and S. Longhi, Phys. Rev. Lett. **104**, 150403 (2010).
17. G. Della Valle and S. Longhi, J. Phys. B **43**, 051002 (2010).
18. I. I. Smolyaninov, Q. Balzano, and C. C. Davis, Phys. Rev. B **72**, 165412 (2005).
19. I. I. Smolyaninov, New J. Phys. **5**, 147 (2003).
20. I. Epstein, Y. Lilach, and A. Arie, J. Opt. Soc. Am. B **31**, 1642 (2014).
21. "Reflow of photoresist," https://www.microchemicals.com/technical_information/reflow_photoresist.pdf.
22. S. Ruschin and E. Marom, J. Opt. Soc. Am. A **1**, 1120 (1984).
23. A. Messiah, *Quantum Mechanics* (North-Holland, 2005).
24. S. I. Bozhevolnyi, V. S. Volkov, E. Devaux, and T. W. Ebbesen, Phys. Rev. Lett. **95**, 046802 (2005).
25. A. Boltasseva, V. S. Volkov, R. B. Nielsen, E. Moreno, S. G. Rodrigo, and S. I. Bozhevolnyi, Opt. Express **16**, 5252 (2008).
26. E. Moreno, S. G. Rodrigo, S. I. Bozhevolnyi, L. Martín-Moreno, and F. J. García-Vidal, Phys. Rev. Lett. **100**, 023901 (2008).
27. R. Bekenstein, J. Nemirovsky, I. Kaminer, and M. Segev, Phys. Rev. X **4**, 011038 (2014).
28. D. Smirnova, S. H. Mousavi, Z. Wang, Y. S. Kivshar, and A. B. Khanikaev, ACS Photon. **3**, 875 (2016).
29. W. B. Lu, W. Zhu, H. J. Xu, Z. H. Ni, Z. G. Dong, and T. J. Cui, Opt. Express **21**, 10475 (2013).
30. M. V. Berry, J. Phys. A **8**, 1952 (1975).
31. R. C. Mitchell-Thomas, O. Quevedo-Teruel, T. M. McManus, S. A. R. Horsley, and Y. Hao, Opt. Lett. **39**, 3551 (2014).
32. T. Zentgraf, Y. Liu, M. H. Mikkelsen, J. Valentine, and X. Zhang, Nat. Nanotechnol. **6**, 151 (2011).
33. C. Sheng, R. Bekenstein, H. Liu, S. Zhu, and M. Segev, Nat. Commun. **7**, 10747 (2016).
34. A. Aubry, D. Y. Lei, A. I. Fernández-Domínguez, Y. Sonnefraud, S. A. Maier, and J. B. Pendry, Nano Lett. **10**, 2574 (2010).
35. T. Zentgraf, J. Valentine, N. Tapia, J. Li, and X. Zhang, Adv. Mater. **22**, 2561 (2010).
36. R. Zuo, W. Liu, H. Cheng, S. Chen, and J. Tian, Adv. Opt. Mater. **6**, 1800795 (2018).
37. W. Liu, Z. Li, H. Cheng, C. Tang, J. Li, S. Zhang, S. Chen, and J. Tian, Adv. Mater. **30**, 1706368 (2018).
38. J. Steinhauer, Nat. Phys. **12**, 959 (2016).